


Monoolein aqueous dispersions as a delivery system for quercetin

Rita Cortesi¹  · Enrica Cappellozza¹ · Markus Drechsler² · Catia Contado³ · Anna Baldisserotto¹ · Paolo Mariani⁴ · Federica Carducci⁴ · Alessandra Pecorelli⁵ · Elisabetta Esposito¹ · Giuseppe Valacchi^{1,5}

Published online: 8 May 2017
© Springer Science+Business Media New York 2017

Abstract This study describes the preparation, characterization and *in vitro* release of monoolein aqueous dispersions (MAD) encapsulating quercetin (QT). As emulsifier, sodium cholate was employed at two different concentrations, namely 0.15% and 0.25% with respect to the total weight of the formulation. Cryogenic Transmission electron microscopy and X-ray analysis indicated that MAD015 are a mixture of vesicles and cubic structures, whilst MAD025 are mainly characterized by unilamellar vesicular structures. Photon correlation spectroscopy (PCS) and Sedimentation Field Flow Fractionation (SdFFF) showed a MAD size higher than 300 nm that over 100 days from analysis reduces up to 200 nm. *In vitro* Franz cell experiments showed that the two systems had a similar behaviour in the release of QT. Experiments on antioxidant activity of MAD containing QT demonstrated that their activity parallel with the content of encapsulated QT within the MAD formulations produced. Taken together these results allow us to conclude that MAD can be potentially proposed for the delivery of QT.

Keywords Quercetin · Monoolein aqueous dispersions (MAD) · Monoolein · Antioxidant activity

Abbreviations

MAD	Monoolein Aqueous Dispersions
cryo-TEM	cryogenic transmission electron microscopy
PCS	photon correlation spectroscopy
SdFFF	Sedimentation Field Flow Fractionation

1 Introduction

Quercetin (3,3¹,4¹,5¹-7-pentahydroxyflavone, QT) is one of the most common dietary flavonoids. Many studies demonstrated that QT has promising use as natural compound in cancer prevention and/or treatment (Avila et al. 1994; Duo et al. 2012). In addition QT possesses a variety of biological activities and pharmacological actions, such as decreasing blood lipid, dilating coronary arteries, anti-oxidation, anti-inflammation, anti-platelet aggregation, anti-anaemic action and anti-anaphylaxis effects (Hollman and Katan 1999). QT is the most commonly investigated flavonoid that presents the highest antiradical property compared to other flavonoids. It has been verified that QT can scavenge free radicals and inhibits lipid peroxidation (Formica and Regelson 1995; Skaper et al. 1997). Therefore, topical application of QT has received considerable attention for the ability of against ROS-mediated damage in the skin (Casagrande et al. 2006, 2007; Vicentini et al. 2008).

However, its application is limited due to its low aqueous solubility (varying from 0.00215 g/L at 25 °C to 0.665 g/L at 140 °C) (Kumari et al. 2012) that contributes to a low absorption *in vivo* (Li et al. 2009; Khaled et al. 2003). To potentially solve these problems and to develop novel vehicle able to

✉ Rita Cortesi
crt@unife.it

¹ Department of Life Sciences and Biotechnology, University of Ferrara, Via Fossato di Mortara, 19, I-44121 Ferrara, Italy
² BIMF / Soft Matter Electronmicroscopy, University of Bayreuth, Bayreuth, Germany
³ Department of Chemical and Pharmaceutical Sciences, University of Ferrara, Ferrara, Italy
⁴ Department of Life and Environmental Sciences, Università Politecnica delle Marche, Ancona, Italy
⁵ Animal Sciences Department, Plants for Human Health Institute, NC State University, NC Research Campus. 600 Laureate Way, Kannapolis, NC 28081, USA

transport QT through the skin, biodegradable and biocompatible nanoparticles have been recently proposed (Aditya et al. 2014; Anwer et al. 2016; Lee et al. 2016). Particularly, in this study monoolein aqueous dispersions have been considered.

It has been proven that lipidic dispersions are matrixes able to dissolve and deliver active molecules in a controlled fashion, thereby improving bioavailability and reducing side effects (Yaghmur and Glatter 2009; Siekmann et al. 2002). Unsaturated long-chain monoglycerides emulsified in water (i.e. monoolein) lead to aqueous nanostructured dispersions (monoolein aqueous dispersions, MAD) of complex lyotropic liquid crystalline phases (lamellar, hexagonal, and cubic structure) (Gustafsson et al. 1996; Esposito et al. 2012). The nature of MAD dispersed phase is influenced by the type of emulsifier (Worle et al. 2007). In this study sodium cholate (Na cholate), the bile salt commonly used for liposome production, was chosen for the production of MAD (Esposito et al. 2013). MAD were produced by standard protocols then characterized in terms of morphology, dimensional distribution and inner structure by means of Cryogenic Transmission Electron Microscopy (cryo-TEM), Photon Correlation Spectroscopy (PCS) and Sedimentation Field Flow Fractionation (SdFFF) (Jores et al. 2004). Moreover, *in vitro* experiments were carried out to evaluate drug content, drug release kinetics antioxidant and cytotoxic activities of MAD-QT.

2 Materials and methods

2.1 Materials

Glyceryl monooleate RYLO MG 19 (monoolein) was a gift from Danisco Cultor (Grindsted, Denmark). Sodium cholate (Na cholate) ($3\alpha,7\alpha,12\alpha$ -Trihydroxy- 5β -cholan-24-oic acid sodium salt), quercetin (QT), DPPH (2,2 diphenyl-picrylhydrazyl) and Folin-Ciocalteu's phenol reagent were purchased from Sigma Chemical Company (St Louis, MO, USA). Solvents were of HPLC grade and all other chemicals of analytical grade were from Sigma-Aldrich (Milano, Italy).

2.2 MAD preparation

Preparation of dispersions was based on the emulsification of monoolein and emulsifier in water, as previously described (Puglia et al. 2013; Esposito et al. 2013). Briefly, after dispersing monoolein and sodium cholate in water, using the ratios reported in Table 1, the dispersion was homogenized (15,000 rev min⁻¹, Ultra Turrax, Janke & Kunkel, Ika-Werk, Sardo, Italy) at 60 °C for 1 min, then cooled and maintained at room temperature in glass vials.

To produce QT containing MAD, 0.25 mg/ml of QT corresponding to 0.5% by weight with respect to the monoolein and

Table 1 Composition of the produced MAD

Component (%w/w)	MAD015	MAD025
Monoolein	4.5	5
Sodium cholate	0.15	0.25
water (HPLC grade)	95.35	94.75

0.025% w/w with respect to the dispersion, was employed. QT was added to the molten monoolein/emulsifier mixture and dissolved before addition to the aqueous solution. Afterwards the dispersion was prepared as above described.

2.3 Characterization of MAD

2.3.1 Cryo-transmission electron microscopy

Samples vitrified as previously described (Esposito et al. 2008) were transferred to a Zeiss EM922Omega transmission electron microscope for imaging using a cryoholder (CT3500, Gatan). Throughout the examination, the sample temperature was kept below -175 °C. Specimens were examined with doses of about 1000–2000 e/nm² at 200 kV. Images recorded by a CCD digital camera (Ultrascan 1000, Gatan, Munich, Germany), were analysed using a GMS 1.8 software (Gatan, Munich, Germany).

2.3.2 X-ray diffraction

X-ray diffraction experiments were performed to characterize the inner structure of MADs. A 3.5 kW Philips PW 1830 X-ray generator (Philips, Eindhoven, The Netherlands) equipped with a home made Guinier-type focusing camera operating in vacuum with a bent quartz crystal monochromator ($\lambda = 1.54$ Å) was used. Diffraction patterns were recorded on a GNR Analytical Instruments imaging plate system (GNR Analytical Instruments Group, Novara, Italy). Samples were held in a tight vacuum cylindrical cell provided with thin mylar windows. Diffraction data were collected at ambient temperature (37 °C), using a Haake F3 thermostat (ThermoHaake, Karlsruhe, Germany) with an accuracy of 0.1 °C.

The spacing of the Bragg peaks detected in the low-angle X-ray diffraction region ($Q < 0.6$ Å⁻¹, being Q the modulus of the scattering vector defined by $Q = 4\pi \sin \theta / \lambda$, where 2θ is the scattering angle) was measured and peak indexing was performed considering the different symmetries commonly observed in lipid phases (Luzzati et al. 1997).

2.3.3 Photon correlation spectroscopy (PCS)

Submicron particle size analysis was performed using a Zetasizer Nano Series, Nano SP90 (Malvern Instr., Malvern,

England) equipped with a 5 mW helium neon laser with a wavelength output of 633 nm. Glassware was cleaned of dust by washing with detergent and rinsing twice with water for injections. Measurements were made at 25 °C at an angle of 90°. Data were interpreted using the CONTIN method (Pecora 2000).

2.3.4 Sedimentation field flow fractionation analysis

A sedimentation field flow fractionation analysis (SdFFF) system (Model S101, FFFractionation, Inc., Salt Lake City, UT, USA) was employed to determine the size distribution of particles by converting the fractograms, i.e. the graphical results (Contado et al. 1997). Fifty microliter samples were injected through a 50 µl Rheodyne loop valve. As mobile phase demineralized water pumped at 2.0 ml/min was used. After the SdFFF system fractions of 3 ml, being the collecting time 90 s, were automatically collected by a Model 2110 fraction collector (Bio Rad laboratories, UK). The volume of each fraction was 3 ml.

2.4 Drug content in MAD

The encapsulation efficiency (EE) of QT in MAD was determined as previously described (Puglia et al. 2013). 100-µl of each MAD batch was loaded in a centrifugal filter (Microcon centrifugal filter unit YM-10 membrane, NMWCO 10 kDa, Sigma Aldrich, St Louis, MO, USA) and centrifuged (Spectrafuge™ 24D Digital Microcentrifuge, Woodbridge NJ, USA) at 8000 rpm for 20 min. The amount of drug in both the lipid and the aqueous phase was determined by UV analyses as below reported. The encapsulation parameter was determined as follows.

$$EE = L_{QT} / T_{QT} \times 100 \quad (1)$$

where L_{QT} is the amount of drug encapsulated in MAD and T_{QT} is the total weight of QT for the MAD preparation.

2.5 Stability studies

Physical and chemical stability studies were conducted in triplicate during hundred days from formulations production.

Physical stability was evaluated by visual inspection analysing the macroscopic aspect (i.e. phase separation, turbidity and macroscopic viscosity) of the formulations, whilst chemical stability was evaluated on drug loaded formulations, stored at 25 °C, determining QT content by UV analyses. Shelf life values were calculated as follows (Esposito et al. 2014).

Log (QT residual content, %) was plotted against time and the slopes (m) were calculated by linear regression. The slopes (m) were then substituted into eq. (2) for the determination of k values:

$$k = m \times 2.303 \quad (2)$$

Shelf life values (the time for 10% loss, t_{90}) were then calculated by the eq. (3):

$$t_{90} = 0.105 / k \quad (3)$$

as previously reported (Wells 1988).

2.6 UV spectroscopy analyses

QT determination was performed using a double-ray UV/Vis spectrometer (UV/VIS/NIR Spectrometer Lambda 19, Perkin Elmer) operating at 375 nm and 1 ml quartz cuvettes. To calculate the QT concentration within each sample a QT calibration curve was previously achieved and used as reference.

2.7 In vitro release profiles studies

In vitro release profiles studies were performed using the Franz type cells supplied by LGA (Berkeley, CA) associated to nylon membrane (Millipore, 0.45 µm pore size).

Nylon membranes were rehydrated by immersion in distilled water at room temperature for 1 h before being mounted in Franz cell. The exposed surface area was 0.78 cm² (the diameter of the orifice was 1 cm). The receptor compartment contained 5 ml of a mixture of phosphate buffer 60 mM pH 7.4 and methanol (50:50, v/v) as above reported. This solution was stirred with the help of a magnetic bar at 500 rpm and thermostated at 32 ± 1 °C during all the experiments (Siewert et al. 2003).

1 ml of each formulation was placed on the membrane surface then the donor compartment was sealed to avoid evaporation. At predetermined time intervals comprised between 1 and 24 h, namely 5 min, 15 min, 30 min, 1 h, 90 min, 2 h, 3 h, 4 h, 5 h, 6 h, 7 h, 8 h and 24 h, samples (0.15 ml) of receptor phase were withdrawn and QT concentration in the receptor phase was measured using UV. Each removed sample was replaced with an equal volume of fresh receptor phase. The QT concentrations were determined three times in independent experiments and the mean values ± standard deviations were calculated. The mean values were then plotted as a function of time.

2.8 Antioxidant activity

2.8.1 Determination of total phenolic content: Folin-Ciocalteu assay

The concentration of QT in MAD was determined using spectrophotometric method (Singleton et al. 1999). Ethanol solution of QT (or gallic acid, used as reference) at known concentration was used in the analysis. The reaction mixture was

prepared by mixing 2 ml of ethanol solution of MAD, 10 ml of 10% Folin-Ciocalteu's reagent dissolved in water and 8 ml 7.5% NaHCO₃. Blank was concomitantly prepared, containing 2 ml ethanol, 10 ml 10% Folin-Ciocalteu's reagent dissolved in water and 8 ml of 7.5% of NaHCO₃. The samples were thereafter incubated at room temperature for 2 h. The absorbance was determined using spectrophotometer at $\lambda_{\max} = 765$ nm. The samples were prepared in triplicate for each analysis and the mean value of absorbance was obtained. The same procedure was repeated for the standard solution of gallic acid and the calibration line was constructed. Based on the measured absorbance, the concentration of phenolics was read (mg/ml) from the calibration line; then the content of phenolics was expressed in terms of gallic acid equivalent.

2.8.2 Free radical scavenging activity on DPPH: DPPH (2,2-diphenyl-1-picrylhydrazyl) assay

The ability of the QT to scavenge DPPH free radicals was assessed by the standard method (Tekao et al. 1994; Kumarasamy et al. 2007). DPPH test is one of the simplest and fastest methods for the evaluation of the antioxidant compounds (Blois 1958) and allows measure of the reducing activity of antioxidant molecules against the DPPH radical by a colorimetric reaction. Indeed DPPH (red-purple coloured) decolorizes in the presence of an antioxidant agent. This assay is able to detect compounds acting for transfer of hydrogen or electrons (radical quenching) and such ability is evaluated by measuring the decrease of absorbance at 517 nm of the solution after the radical reaction with the products to be tested.

The percentage of radical scavenging capacity was calculated using eq. (4):

DPPH radical-scavenging capacity (%)

$$= \left[1 - \frac{(A1 - A2)}{A0} \right] \times 100 \quad (4)$$

where A0 is the absorbance of the control (without QT), A1 is the absorbance in the presence of the QT, and A2 is the absorbance without DPPH.

To a methanol solution of DPPH (1.5 mL) 0.750 mL of QT (solution or MAD) at different concentration were added. The absorbance at 517 nm was measured by a UV-VIS spectrophotometer (Beckman Coulter™, DU@530, Life Science UV/VIS spectrophotometer, Single Cell Module) according to a described procedure (Wang et al. 1998). Results were expressed as $\mu\text{mol Trolox equivalent/g}$ of compounds.

2.9 Cytotoxicity determination

Human keratinocytes HaCaT cells were cultured in Dulbecco's modified Eagle's medium High Glucose (Lonza, Milan, Italy), supplemented with 10% FBS,

100 U/ml penicillin, 100 $\mu\text{g/ml}$ streptomycin and 2 mM L-glutamine, at 37 °C in a 5% CO₂ humidified atmosphere.

The cells were grown to confluence in 96-well tissue culture plate and then treated with the different doses of both MAD025-QT and MAD015-QT, in the range of 0.1 to 10 μM of QT. 100 μM QT stock solutions for both MAD were diluted to the required concentrations directly in the medium. Cytotoxicity was determined 24 h after the treatments by LDH assay (EuroClone, Milan, Italy). Briefly, the culture media were collected and LDH release was measured by enzymatic assay: in the first step NAD⁺ is reduced to NADH/H⁺ by the LDH-catalyzed conversion of lactate to pyruvate; in the second step the catalyst (diaphorase) transfers H/H⁺ from NADH/H⁺ to tetrazolium salt which is reduced to formazan. To induce the total release of intracellular LDH, some wells of HaCaT were treated with 1% Triton X-100. The amount of LDH in the supernatant were determined and calculated according to kit instructions. The degree of LDH release in each sample was determined by measuring the absorbance at 490 nm using a microplate spectrophotometer. The absorbance measured from three wells was averaged, and the percentage of LDH released was calculated as percentage of change relative to 1% Triton X-100 treated cells. All tests were performed in triplicate and repeated at least three times.

Statistical analysis was performed by unpaired two-tailed t test (GraphPad Prism software, San Diego, CA, USA). *P* values <0.05 were considered to be statistically significant.

3 Results and discussion

3.1 Preparation of MAD

In the present study MAD were investigated as nanotechnology systems for QT delivering. Formulations were prepared by emulsifying monoolein in water (Gustafsson et al. 1996; Larsson 2000; Siekmann et al. 2002). It has been shown that the type of emulsifier can influence the nanostructure of MAD disperse phase (Yaghmur and Glatter 2009). Indeed, some emulsifiers used to stabilize cubosomes (i.e. poloxamer 407) display relevant toxicity toward different cell lines (Murgia et al. 2010) due to synergistic action between poloxamer 407 and monoolein. To avoid this cytotoxic effect, sodium cholate (the bile salt commonly used for liposome production) was considered for the production of MAD (Esposito et al. 2013). As summarized in Table 1, two different concentration of sodium cholate were considered, namely 0.15% (MAD015) and 0.25% (MAD025) with respect to the total weight of the formulation.

The concentration of QT employed was 0.25 mg/ml in the final volume of the formulation, corresponding to 0.5% by

weight with respect to the monoolein and 0.025% w/w with respect to the dispersion.

Figure 1 shows the macroscopic aspect of both QT containing MAD015 and MAD025. The formulations appear translucent and homogeneous, yellow coloured due to the presence of QT.

3.2 Characterization of dispersions

3.2.1 Cryo-TEM

In order to shed light on the general morphology of the MAD particles, Cryo-TEM analyses were conducted. Figure 2 shows cryo-TEM images of MAD015 (left column) and MAD025 (right column). MAD015 are characterized by a miscellaneous of structures, namely vesicles and cubic structures. In particular, in the left column, unilamellar invaginated vesicles can be observed together with cubosomal structures. The presence of cubic structures could be responsible for the viscous aspect to the formulation. No significant differences are appreciable between empty (Fig. 2A) and QT loaded MAD (Fig. 2C, F) indicating that the presence of the QT does not affect the aspect of MAD. On the other hand MAD025 are mainly characterized by unilamellar vesicular structures both in the absence (Fig. 2B) and in the presence of QT (Fig. 2D,E). The presence of a vesicular dispersion gives rise to the macroscopic aspect of the formulation and to its fluidity. The black dots are ascribed to ice crystals contamination due to sample preparation. As it is possible to observe from panels of the right column, the presence of QT does not seem to affect MAD aspect.

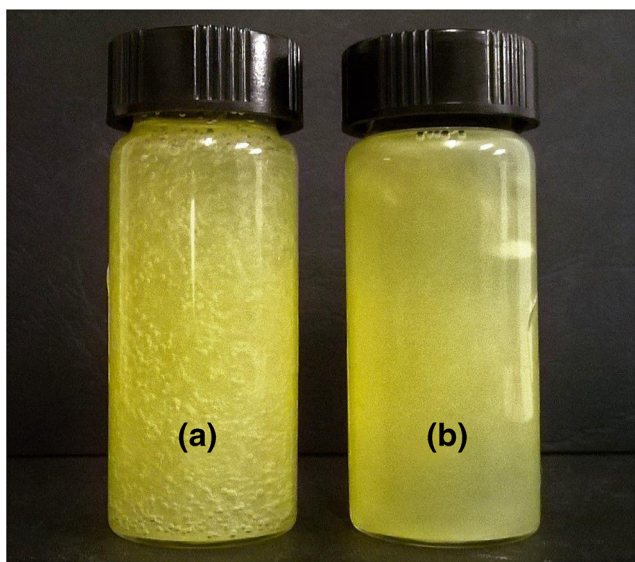


Fig. 1 Macroscopic aspect of the produced MAD: MAD015QT (a) and MAD025QT (b)

3.2.2 X-ray diffraction

X-ray diffraction analysis allowed the investigation of the inner structural organization of MADs. Experiments were conducted at 37 °C on both MAD015 and MAD025 with or without QT. The X-ray diffraction profiles for MAD025, both in the absence and in the presence of QT, did not show detectable signals, suggesting the eventual presence of very small cubosomes. On the other hand, the X-ray diffraction profiles observed in the case of MAD015 indicate the presence of cubosomes with an Im3m cubic structure (see Fig. 3) (Mariani et al. 1988). However, the unit cell parameter depends on the presence of QT: for empty MAD015, the unit cell was $a = 153.4 \text{ \AA}$ while for MAD015QT, the unit cell was $a = 137.9 \text{ \AA}$. Therefore, no changes have been detected in the inner structure of the monoolein cubosomes, even if QT appears to induce a small shrinking of the water channels probably determined by surface dehydration.

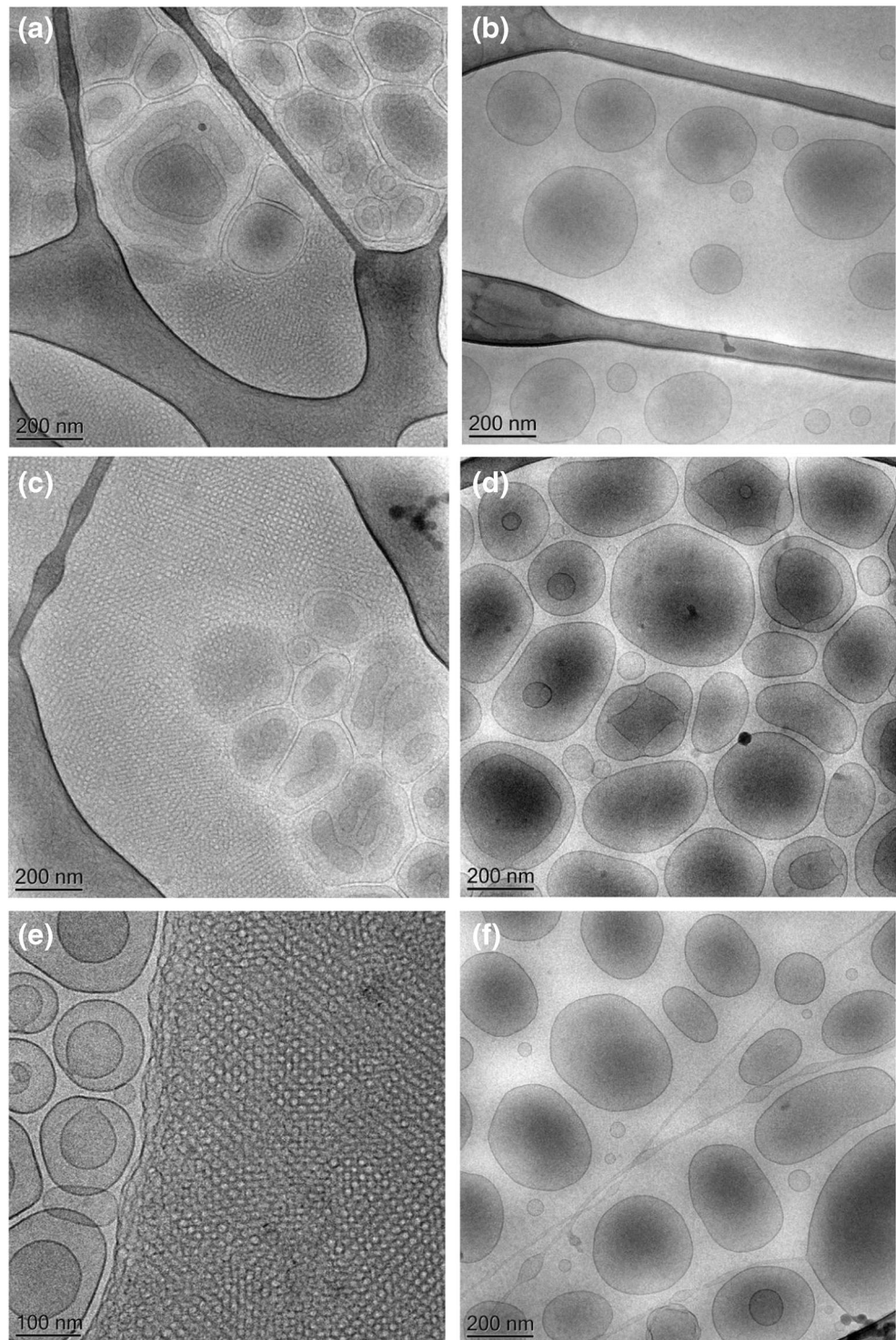
3.2.3 PCS and SdFFF analyses

Table 2 reports the dimensional size distribution of empty and QT loaded MAD during time as determined by PCS measurements. It was found that the presence of QT induces an increase in the mean diameter of MAD015QT and MAD025QT as compared to that of the corresponding MAD without drug probably due to its disposition within the lipids. Particularly, MAD015QT and MAD025QT showed an initial Z-average mean diameter of 402.3 and 321.6 nm, respectively, while empty MAD015 and MAD025 showed an initial Z-average mean diameter of 227.3 and 230.2 nm. From these results it emerges that the higher the concentration of sodium cholate the lower the mean size. This behaviour could be ascribed to the intercalation of the emulsifiers between the molecules of the lipid that induces the formation of smaller particles and mixed micelles. In all cases the mean diameter tends to reduce during time possibly due to a rearrangement of sodium cholate molecules within the lipid structures leading to the formation of a lower entropy system.

MADQT size distribution was also determined by SdFFF method. This method allows us to measure the particle size distribution within the sample, by retaining particles of different diameter and eluting them at a calculable time (Merkus et al. 1989). Indeed an observed retention time can be directly related by theory to the mass of the eluting particles and transformed into a size. On the other hand the UV signal can be transformed into a mass frequency function (Contado et al. 1997; Esposito et al. 2008). The obtained fractograms are converted into size distribution plots according to well-proven equations.

Since particle in SdFFF sort based on their specific mass, knowing the particle density and supposing a spherical shape, the sizes represent diameter of an equivalent

Fig. 2 Cryo-transmission electron microscopy images (cryo-TEM) of MAD015 (left column) and MAD025 (right column). Micrographs refer to empty MAD015 (a) and MAD025 (b) and to MAD015QT (c, e) and MAD025QT (d, f)



sphere (Bunjés 2005). The MAD density was calculated as previously reported by Esposito et al. (2015). In Fig. 4 the PSD plots of MAD025QT and MAD015QT are reported. The samples are characterized by a size distribution superimposable to that obtained by PCS. PCS and SdFFF are based on different rational principles. Indeed, PCS assesses the size considering the diffusion of the scattered light,

thus the obtained results depend on the position that the particles have when are hit by the laser ray. For data evaluation, the spherical shape is assumed thus uncertainties may result from non-spherical particle shapes. On the other hand SdFFF in some extent “weighs” the particles being thus considered as compact spheres of uniform density. In this respect the complementary evaluation of size

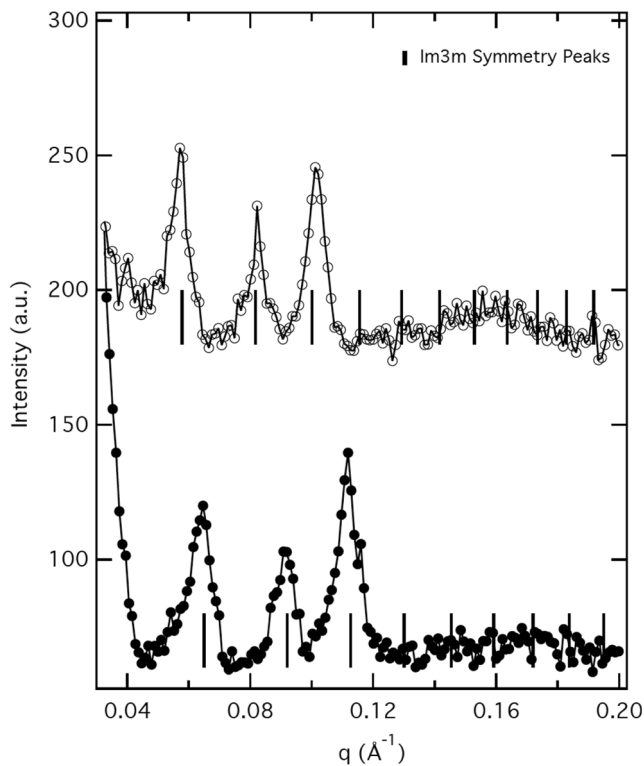


Fig. 3 X-ray diffraction profiles of MAD015 (white circles) and MAD015-QT (black circles)

distribution by mean of PCS and SdFFF lead to realistic information about particle size.

SdFFF was also employed to obtain information about the QT encapsulation. QT’s amount was determined by UV using the eluate exiting from the SdFFF channel collected during the fractionation. The results reported in Fig. 4 (square dots) clearly show that the QT is entirely associated to MAD.

3.3 Stability studies

QT content was monitored up to hundred days from MAD preparations. QT content of both formulations, expressed as percentage of the total amount used for the preparation as a function of time is summarized in Table 3. It was found that

Table 2 Dimensional size (Z-average) of the produced MAD during time as determined by PCS

Time (days)	MAD015 (empty)	MAD015 (QT 0.25 mg/ml)	MAD025 (empty)	MAD025 (QT 0.25 mg/ml)
1	230.3 ± 3.9	402.3 ± 57.9	227.2 ± 2.3	321.6 ± 57.3
7	n.d.	383.9 ± 39.6	n.d.	327.5 ± 26.7
15	227.8 ± 2.7	316.2 ± 40.5	226.6 ± 3.9	297.1 ± 31.9
30	228.3 ± 4.6	283.0 ± 15.3	221.3 ± 3.6	279.4 ± 17.6
100	218.6 ± 2.8	197.4 ± 41.0	212.5 ± 2.3	276.7 ± 8.6

n.d.: not determined

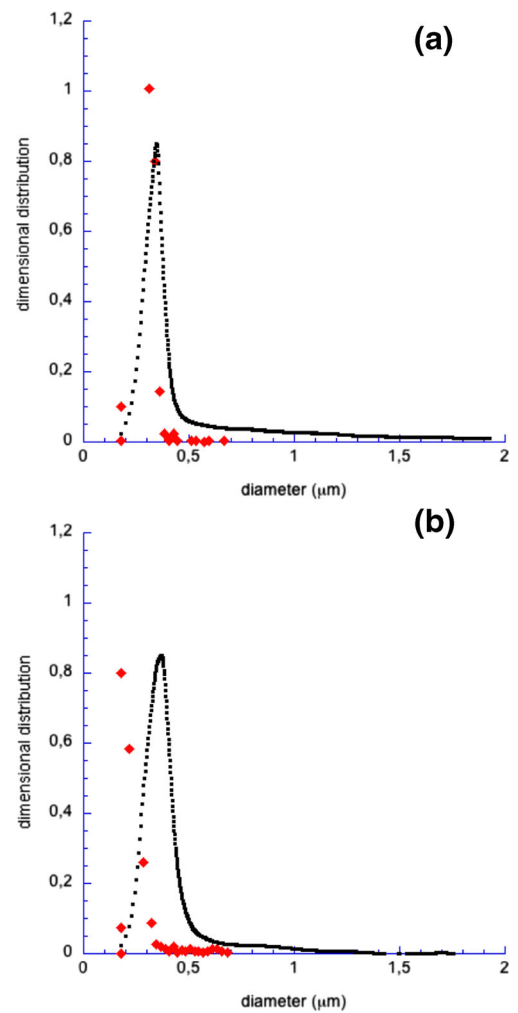


Fig. 4 Size distribution plots of MAD015QT (a) and MAD025QT (b) elaborated from the SdFFF fractograms. The dots indicate QT content, as determined by UV

the encapsulation efficiency (EE) is $90.5 \pm 18.0\%$ for MAD015 and $84.4 \pm 11.8\%$ for MAD025. During time both preparation showed a decrease in QT content up to 63.5% and 77% for MAD015 and MAD025, respectively.

Shelf life stability was calculated plotting Log QT residual content (i.e. the % with respect to drug content at time 0) against time, obtaining first order kinetics (data not shown).

Table 3 QT content in MAD as a function of time

QT recovery (%) ^a			
Time (days)	QT (ethanol solution)	MAD015QT	MAD025QT
1	99.10 ± 1.4	99.85 ± 1.2	99.91 ± 1.4
7	97.62 ± 2.9	94.66 ± 3.8	96.34 ± 3.8
15	96.91 ± 3.5	90.5 ± 8.0	94.4 ± 11.8
30	74.32 ± 2.8	82.3 ± 2.5	88.5 ± 16.3
60	68.2 ± 6.4	72.3 ± 14.0	74.4 ± 21.3
90	n.d.	73.3 ± 8.4	73.0 ± 31.7
100	n.d.	63.5 ± 10.0	67.0 ± 8.5
Shelf life values			
<i>K</i>	0.0070697	0.0063559	0.0038649
<i>t</i> ₉₀ (days) ^b	14.84	16.52	27.17
<i>t</i> _{1/2} (days) ^c	98.02	109.03	179.31

a: as a function of initial QT content by weight.

b: Time at which the drug concentration has lost 10%.

c: Time at which the drug concentration has lost 50%

The reported results represent the average of four independent experiments ± s.d.

n.d.: not determined

From the slopes (*m*), obtained by linear regression, shelf life values (*t*₉₀) and (*t*_{1/2}), i.e. the time at which the drug concentration has lost 10% or 50% respectively, were calculated and reported in Table 3. It was found that MAD015QT maintains 90% of QT stability for 16 days and 50% stability for 109 days, whilst in the case of MAD025QT *t*₉₀ was almost 27 days and *t*_{1/2} 179 days.

From the analysis of these data, the shelf-life of QT in MAD is comparable to that of QT in ethanol solution (*t*₉₀: 14.84 days and *t*_{1/2}: 98.02 days). Particularly, the longest *t*₉₀ and *t*_{1/2} were found for MAD015QT being around 27 and 179 days, respectively. It is evident that for a pharmaceutical use these results, being a too short period of time, do not give sufficient improvement of QT stability, thus further studies aimed to reach this goal have to be performed in the future evaluating different composition of MAD. However, it should be underlined that the present study allowed the obtaining of a formulation in which QT is “solubilized” in water at a concentration up to 20 fold higher than the maximum solubility of QT in water reported in literature (Gao et al. 2011), leading therefore to an increase of incorporation of QT into water-based matrix.

3.4 In vitro studies

3.4.1 Drug release experiments

For comparing the release of QT from the two MAD formulations, Franz-cells associated to nylon membrane were

used. Nylon membrane retained MAD and allowed the transfer of the drug immediately into the receiving compartment. Since the QT is poorly soluble in water, its release in aqueous physiological receptor phases is undetectable. Therefore a non-physiological receptor phase with 30% by volume of ethanol was used in order to allow the establishment of the sink conditions and to sustain permeant solubilization (Siewert et al. 2003; Liu et al. 2014).

In Fig. 5 the cumulative plots of the amount of QT permeated through nylon membrane as a function of time are reported. From the obtained release profiles it is evident that the two systems displayed a similar behaviour in controlling the release of QT.

3.4.2 Antioxidant activity

It is well known that various pathophysiological processes are due to the presence of free radicals, thus the antioxidant intervention is of pivotal importance. In this view, MAD015QT and MAD025QT were tested to determine the antioxidant capacity of QT by mean of Folin-Ciocalteu analysis and DPPH assay. The results, expressed as Gallic Acid Equivalents (GAE) in the first case and in μmol TE/g in the second case, are summarized in Table 4.

Colorimetric reactions are widely used in the UV/VIS spectrophotometric method as rapid and applicable in routine laboratory use (Pelozo et al. 2008). QT in the sample

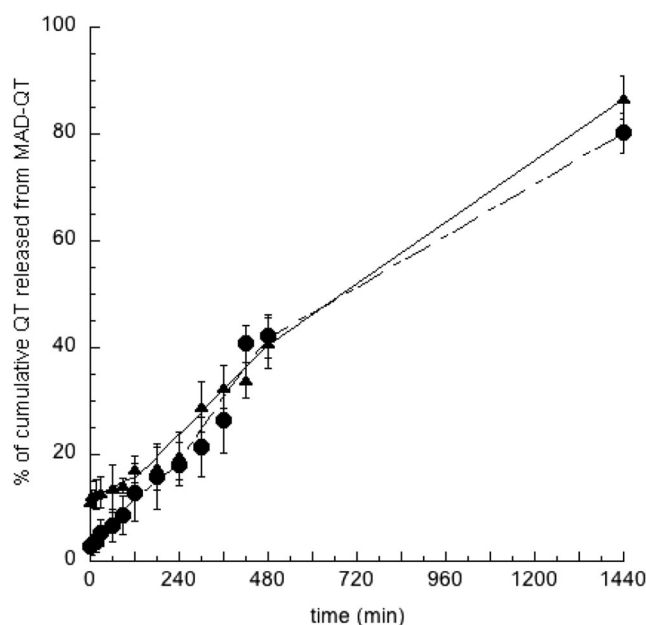


Fig. 5 In vitro release profile of QT from MAD015QT (triangles) and MAD025QT (circles). Experiments were performed by Franz cell method. Data were the mean of 3 independent experiments ± s.d

Table 4 Antioxidant activity of QT containing MAD as determined by Folin-Ciocalteu and DPPH assays

Antioxidant test	MAD015-QT	MAD025-QT
Folin-Ciocalteu ^a	2.2 ± 0.6	3.5 ± 0.4
DPPH ^b	1.686 ± 0.055	1.557 ± 0.042

^a GAE_{QT} = 1.32 mg/L

^b DPPH unit = μmol Trolox equivalents/g

react with specific redox reagents (Folin-Ciocalteu reagent) to form a blue complex that can be quantified by visible-light spectrophotometry (Schofield et al. 2001). However, colorimetric assay need to use a reference substance. In the present study gallic acid was considered as reference. It was found that MAD015QT displayed an activity of 2.2 GAE, whilst MAD025QT an activity of 3.5 (Table 4).

Concerning DPPH assay, the antioxidant activity was assessed based on the scavenging activity of the stable DPPH free radical. The effect of QT on DPPH radical scavenging is well known. The effect of QT as antioxidant on DPPH radical scavenging is thought to be due to its hydrogen-donating ability. Indeed, the radical scavenging activity of flavonoids toward DPPH radicals depends on the number of hydroxyl groups (Soares et al. 1997). The greater the number of hydroxyl groups, the greater the radical-scavenging potency of flavonoids (Cao et al. 1993). It was found that MAD015QT and MAD025QT displayed a comparable activity being 1.686 and 1.557 DPPH units, respectively (Table 4). These values are the 81,06% and 74,85% of the DPPH activity of a QT solution 0.025% p/v (namely 2.08 DPPH units), thus are in agreement with the content of encapsulated QT within the MAD formulations produced.

3.4.3 Effect on human keratinocytes

To test whether QT containing MAD015 and MAD025 could be toxic to the cells, a LDH assay was carried out, which measures LDH activity released in the medium from the cytosol of damaged cells. As it is shown in Fig. 6, there was a dose-dependent increase of LDH activity with both formulations at concentrations above 1 μM (i.e. 0.030% w/w) of QT compared to the control cells. No significant difference was observed among control and MAD treated cells at 0.1 and 0.5 μM QT containing MAD (Fig. 6). This indicates that MAD encapsulating QT does not cause acute cytotoxicity at concentrations below 1 μM of QT.

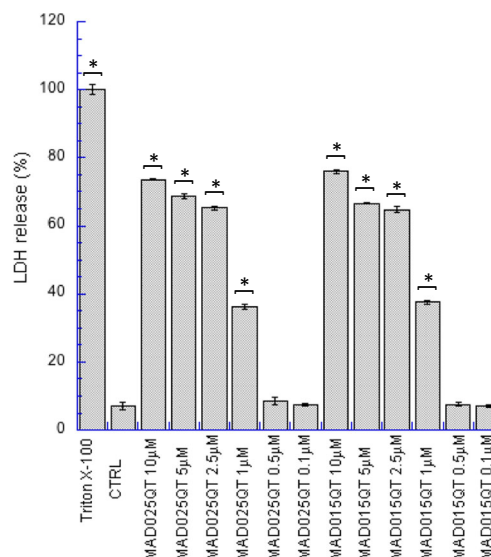


Fig. 6 Toxicity of MAD indicated by the amount of lactate dehydrogenase (LDH) released from HaCaT cells treated for 24 h with the tested products at different concentrations. Each value indicates the percentage level of LDH released after treatment with the specific dose of product, relative to the concentration of LDH released after treatment with Triton X-100. Data are the mean of three independent experiments ± s.d. conducted in triplicate. * $p < 0.05$

4 Conclusions

This study indicates that MAD can be used as a tool to transport QT in order to overcome its low aqueous solubility. Particularly, the selected emulsifier sodium cholate, employed at two different concentrations (i.e., 0.15% and 0.25%), gave rise to formulations characterized by an antioxidant activity comparable to that of free QT solution used at the same concentration.

Cryo- TEM and X-ray indicated that the content of the emulsifier influences the morphological aspect of the MAD. Indeed MAD015 is a mixture of vesicles and cubic structures, whilst MAD025 is mainly characterized by unilamellar vesicular structures. In all cases, as evidenced by SdFFF, QT is almost completely associated to the dispersed phase of the formulation. *In vitro* Franz cell experiments showed that the two systems displayed a similar behaviour in controlling the release of QT. Taken together the results described in the present study and the therapeutic properties of QT it is possible to potentially propose MAD for the solubilization and delivery of QT. However, despite many studies still need to be conducted, the possibility to include MAD-containing QT in aqueous based formulations (such as hydrophilic gels) represent a potential breakthrough to obtain semisolid products to be applied on the skin in order to treat some disorders, such as psoriasis or dermatitis (Vijayalakshmi et al. 2012; Karuppagounder et al. 2016; Park et al. 2015).

Acknowledgements Authors are grateful to Dr. M. Sguizzato and Dr. G. Pavoni for technical issues. F.C. acknowledges support from Italian FIRB “Future in research” RBFR12SIPT MIND. The authors thank the CAMERA DI COMMERCIO, INDUSTRIA, ARTIGIANATO E AGRICOLTURA (CCIAA) of Ferrara BANDO ANNO 2015 project for financial support.

References

- N.P. Aditya, A.S. Macedo, S. Doktorovova, E.B. Souto, S. Kim, P.S. Chang, S. Ko, Development and evaluation of lipid nanocarriers for quercetin delivery: a comparative study of solid lipid nanoparticles (SLN), nanostructured lipid carriers (NLC), and lipid nanoemulsions (LNE). *LWT - Food Sci. Technol.* **59**, 115–121 (2014)
- M.K. Anwer, M.A. Al-Mansoor, S. Jamil, R. Al-Shdefat, M.N. Ansari, F. Shakeel, Development and evaluation of PLGA polymer based nanoparticles of quercetin. *Int. J. Biol. Macromol.* **92**, 213–219 (2016)
- M.A. Avila, J.A. Velasco, J. Cansado, V. Notario, Quercetin mediates the down-regulation of mutant p53 in the human breast cancer cell line MDA-MB468. *Cancer Res.* **54**, 2424–2427 (1994)
- M.S. Blois, Antioxidant determinations by the use of a stable free radical. *Nature* **181**, 1199–1200 (1958)
- H. Bunjes, in *Lipospheres in drug targets and delivery: approaches, methods and applications*, ed. By C. Nastruzzi (CRC Press, New York, 2005), pp 41–66.
- G. Cao, H.M. Alessio, R.G. Cutler, Oxygen-radical absorbance capacity assay for antioxidants. *Free Rad. Biol. Med.* **14**, 303–311 (1993)
- R. Casagrande, S.R. Georgetti, W.A. Verir Jr., D.J. Dorta, A.C. dos Santos, M.J. Fonseca, Protective effect of topical formulations containing quercetin against UVB-induced oxidative stress in hairless mice. *J. Photochem. Photobiol. B* **84**, 21–27 (2006)
- R. Casagrande, S.R. Georgetti, W.A. Verir Jr., M.F. Borin, R.F. Lopez, M.J. Fonseca, In vitro evaluation of quercetin cutaneous absorption from topical formulations and its functional stability by antioxidant activity. *Int. J. Pharm.* **328**, 183–190 (2007)
- C. Contado, G. Blo, F. Fagioli, F. Dondi, R. Beckett, Characterization of river Po particles by sedimentation field-flow fractionation coupled to GFAAS and ICP-MS. *Coll. Surf. A* **120**(47–59) (1997)
- J. Duo, G.G. Ying, G.W. Wang, L. Zhang, Quercetin inhibits human breast cancer cell proliferation and induces apoptosis via Bcl-2 and Bax regulation. *Mol. Med. Rep.* **5**, 1453–1456 (2012)
- E. Esposito, M. Fantin, M. Marti, M. Drechsler, L. Paccamiccio, P. Mariani, E. Sivieri, F. Lain, E. Menegatti, M. Morari, R. Cortesi, Solid lipid nanoparticles as delivery systems for bromocriptine. *Pharm. Res.* **25**, 1521–1530 (2008)
- E. Esposito, P. Mariani, L. Ravani, C. Contado, M. Volta, S. Bido, M. Drechsler, S. Mazzoni, E. Menegatti, M. Morari, R. Cortesi, Nanoparticulate lipid dispersions for bromocriptine delivery: characterization and in vivo study. *Eur. J. Pharm. Biopharm.* **80**(306–312) (2012)
- E. Esposito, L. Ravani, P. Mariani, C. Contado, M. Drechsler, C. Puglia, R. Cortesi, Curcumin containing monoolein aqueous dispersions: a preformulative study. *Mater. Sci. Eng. C* **33**, 4923–4934 (2013)
- E. Esposito, L. Ravani, P. Mariani, N. Huang, P. Boldrini, M. Drechsler, G. Valacchi, R. Cortesi, C. Puglia, Effect of nanostructured lipid vehicles on percutaneous absorption of curcumin. *Eur. J. Pharm. Biopharm.* **86**, 121–132 (2014)
- E. Esposito, L. Ravani, M. Drechsler, P. Mariani, C. Contado, J. Ruokolainen, P. Ratano, P. Campolongo, V. Trezza, C. Nastruzzi, R. Cortesi, Cannabinoid antagonist in nanostructured lipid carriers (NLCs): design, characterization and in vivo study. *Mater. Sci. Eng. C* **48**(328–336) (2015)
- J.V. Formica, W. Regelson, Review of the biology of quercetin and related bioflavonoids. *Food Chem. Toxicol.* **33**(1061–1080) (1995)
- L. Gao, G. Liu, X. Wang, F. Liu, Y. Xu, J. Ma, Preparation of a chemically stable quercetin formulation using nanosuspension technology. *Int. J. Pharm.* **404**, 231–237 (2011)
- J. Gustafsson, H. Ljusberg-Wharen, M. Almgren, K. Larsson, Cubic lipid/water phase dispersed into submicron particles. *Langmuir* **12**, 4611–4613 (1996)
- P.C.H. Hollman, M.B. Katan, Dietary flavonoids: Intake, health effects and bioavailability. *Food Chem. Toxicol.* **37**, 937–942 (1999)
- K. Jores, W. Mehnert, M. Drechsler, H. Bunjes, C. Johann, K. Maeder, Investigations on the structure of solid lipid nanoparticles (SLN) and oil-loaded solid lipid nanoparticles by photon correlation spectroscopy, field-flow fractionation and transmission electron microscopy. *J. Control. Release* **95**, 217–227 (2004)
- V. Karuppagounder, S. Arumugam, R.A. Thandavarayan, R. Sreedhar, V.V. Giridharan, K. Watanabe, Molecular targets of quercetin with anti-inflammatory properties in atopic dermatitis. *Drug Discov. Today* **21**, 632–639 (2016)
- K.A. Khaled, Y.M. El-Sayed, B.M. Al-Hadiya, Disposition of the flavonoid quercetin in rats after single intravenous and oral doses. *Drug Dev. Ind. Pharm.* **29**, 397–403 (2003)
- Y. Kumarasamy, M. Byres, P.J. Cox, M. Jasapars, L. Nahar, S.D. Sarker, Screening seeds of some Scottish plants for free-radical scavenging activity. *Phytother. Res.* **21**, 615–621 (2007)
- A. Kumari, V. Kumar, S.K. Yadav, Plant extract synthesized PLA nanoparticles for controlled and sustained release of quercetin: a green approach. *PLoS One* **7**, e41230 (2012)
- K. Larsson, Aqueous dispersion of cubic lipid/water phases. *Curr. Opin. Colloid Interf. Sci.* **5**, 64–69 (2000)
- G.H. Lee, S.J. Lee, S.W. Jeong, H.-C. Kim, G.Y. Park, S.G. Lee, J.H. Choi, Antioxidative and antiinflammatory activities of quercetin-loaded silica nanoparticles. *Coll. Surf. B* **143**, 511–517 (2016)
- H.L. Li, X.B. Zhao, Y.K. Ma, G.X. Zhai, L.B. Li, H.X. Lou, Enhancement of gastrointestinal absorption of quercetin by solid lipid nanoparticles. *J. Control. Release* **133**, 238–244 (2009)
- L. Liu, Y. Tanga, C. Gao, Y. Li, S. Chen, T. Xiong, J. Li, M. Du, Z. Gong, H. Chen, L. Liu, P. Yao, Characterization and biodistribution in vivo of quercetin-loaded cationic nanostructured lipid carriers. *Coll. Surf. B* **115**, 125–131 (2014)
- V. Luzzati, H. Delacroix, T. Gulik-Krzywicki, P. Mariani, R. Vargas, The cubic phases of lipids. *Curr. Top. Membr.* **44**, 3–7 (1997)
- P. Mariani, V. Luzzati, H. Delacroix, Cubic phases of lipid containing systems. Structure analysis and biological implications. *J. Mol. Biol.* **204**, 165–189 (1988)
- H.G. Merkus, Y. Mori, B. Scarlett, et al., *Coll. Polym. Sci.* **267**, 1102–1110 (1989)
- S. Murgia, A.M. Falchi, M. Mano, S. Lampis, R. Angius, A.M. Carnerup, J. Schmidt, G. Diaz, M. Giacca, Y. Talmon, M. Monduzzi, Nanoparticles from lipid-based liquid crystals: emulsifier influence on morphology and cytotoxicity. *J. Phys. Chem. B* **114**, 3518–3525 (2010)
- E.J. Park, J.Y. Kim, M.S. Jeong, K.Y. Park, K.H. Park, M.W. Lee, S.S. Joo, S.J. Seo, Effect of topical application of quercetin-3-O-(2"-galate)- α -l-rhamnopyranoside on atopic dermatitis in NC/Nga mice. *J. Dermatol. Sci.* **77**, 166–172 (2015)
- R. Pecora, Dynamic light scattering measurement of nanometer particles in liquids. *J. Nanopart. Res.* **2**, 123–131 (2000)
- M.I.G. Pelozo, M.L.C. Cardoso, J.C.P. Mello, et al., *Braz. Arch. Biol. Technol.* **51**, 447–451 (2008)
- C. Puglia, V. Cardile, A.M. Panico, L. Craschi, A. Offerta, S. Caggia, M. Drechsler, P. Mariani, R. Cortesi, E. Esposito, Evaluation of monooleine aqueous dispersions as tools for topical administration

- of curcumin: characterization, in vitro and ex-vivo studies. *J. Pharm. Sci.* **102**, 2349–2361 (2013)
- P. Schofield, D.M. Mbugua, A.N. Pell, Analysis of condensed tannins: a review. *Anim. Feed Sci. Tech.* **91**, 21–40 (2001)
- B. Siekmann, H. Bunjes, M.H.J. Koch, K. Westesen, Preparation and structural investigations of colloidal dispersions prepared from cubic monoglyceride/water phases. *Int. J. Pharm.* **244**, 33–43 (2002)
- M. Siewert, J. Dressman, C.K. Brown, V.P. Shah, FIP/AAPS guidelines to dissolution/in vitro release testing of novel/special dosage forms. *AAPS PharmSciTech* **4**, E7 (2003)
- V.L.E. Singleton, R. Orthofer, R.M. Lamuela-Raventós, Oxidants and antioxidants part a. *Methods Enzymol.* **299**, 152–178 (1999)
- S.D. Skaper, M. Fabris, V. Ferrari, M.D. Carbonare, A. Leon, Quercetin protects cutaneous tissue-associated cell types including sensory neurons from oxidative stress induced by glutathione depletion: Cooperative effects of ascorbic acid. *Free Radic. Biol. Med.* **22**, 669–678 (1997)
- J.S. Soares, T.C.P. Dins, A.P. Cunha, L.M. Almerida, Antioxidant activity of some extracts of thymus zygis. *Free Radic. Res.* **26**(469–472) (1997)
- T. Tekao, N. Watanabe, I. Yagi, K. Sakata, A simple screening method for antioxidant and isolation of several antioxidants produced by marine bacteria from fish and shellfish. *Biosci. Biotechnol. Biochem.* **58**, 1780–1783 (1994)
- F.T. Vicentini, T.R. Simi, J.O. Del Ciampo, N.O. Wolga, D.L. Pitol, M.M. Iyomasa, M.V. Bentley, M.J. Fonseca, Quercetin in w/o microemulsion: in vitro and in vivo skin penetration and efficacy against UVB-induced skin damages evaluated in vivo. *Eur. J. Pharm. Biopharm.* **69**, 948–957 (2008)
- A. Vijayalakshmi, V. Ravichandiran, M. Velraj, S. Nirmala, S. Jayakumari, Screening of flavonoid “quercetin” from the rhizome of *Smilax china* Linn. for anti-psoriatic activity. *Asian Pac. J. Trop. Biomed.* **2**, 269–275 (2012)
- M. Wang, J. Li, M. Rangarajan, Y. Shao, E.J. La Voie, T.-C. Huang, C.-T. Ho, Antioxidative phenolic compound from sage (*Salvia officinalis*). *J. Agric. Food Chem.* **46**, 4868–4873 (1998)
- J.I. Wells, *Pharmaceutical Preformulation: the physicochemical properties of drug substances* (Ellis Horwood, Chichester, 1988)
- G. Worle, M. Drechsler, M.H.J. Koch, B. Siekmann, K. Westesen, H. Bunjes, Influence of composition and preparation parameters on the properties of aqueous monoolein dispersions. *Int. J. Pharm.* **329**, 150–157 (2007)
- A. Yaghmur, O. Glatter, Characterization and potential applications of nanostructured aqueous dispersions. *Adv. Coll. Interf. Sci.* **147-148**, 333–342 (2009)